Available online at www.sciencedirect.com
SCIENCE DIRECT®
Journal of Magnetic Resonance 161 (2003) 215–221
JMR Journal of Magnetic Resonance
www.elsevier.com/locate/jmr

Generalization of the lineshape useful in magnetic resonance spectroscopy

David F. Howarth, John A. Weil,* and Zbigniew Zimpel[1]

Department of Chemistry, 110 Science Place, University of Saskatchewan, University of Saskatchewan, Saskatoon, SK, Canada S7N 5C9

Received 11 October 2002; revised 27 November 2002

Abstract

A new lineshape function is derived from the Tsallis distribution to describe electron paramagnetic resonance (EPR) spectra, and possibly nuclear magnetic resonance (NMR) spectra as well. This lineshape generalizes the Gaussian and Lorentzian lineshapes that are widely used in simulations. The main features of this lineshape function are presented: the normalization, moments, and first derivative. A number of experimental EPR spectra are compared with the results of simulations employing the new lineshape function. The results show that the new lineshape often provides a better approximation of the experimental spectrum. It is also shown that the new parameter of the lineshape function can be used to quantify the intermolecular spin–spin interactions.

Keywords: Tsallis distribution; Lineshape; Magnetic resonance; Spectral simulation

1. Introduction

Ever since measurements of electron paramagnetic resonance (EPR) signals were initially measured and analyzed, their lineshape has typically been assumed to be either Lorentzian or Gaussian. These lines not only have a simple form and desired properties, but also a theoretical basis for their use had been established. A brief review (150+ references), summarizing the development and progress of the art of computer simulation of EPR (and NMR) spectra, is available in the literature [1].

The Lorentzian lineshape is justified by the linear response theory [2]. Here one assumes that the net magnetization of the sample oscillates harmonically in the external magnetic field **B**. In the presence of heuristic dissipation terms describing the transport of energy from the spin system to the heat sink, the linear response to the electromagnetic (microwave) radiation ($\mathbf{B}_\mu$) results in an exponential decay of the magnetization following an electromagnetic field pulse, or to a Lorentzian lineshape of absorption lines in a continuous-wave EPR (or NMR) absorption measurement.

The Gaussian lineshape appears as a result of the inhomogeneity of the resonance field present at each paramagnetic center. Thus, besides inhomogeneity of the external magnetic field, local stresses, and material imperfections cause all the paramagnetic centers absorbing magnetic energy from an electromagnetic field to experience a slightly different interaction with neighboring atoms [3]. These interactions determine the local magnetic field "seen" by each center, and hence the resonance frequency of each center. Statistically, the resonance frequencies of individual magnetization vectors can be described by identical distributions with a finite variance. Each center contributes to the net absorption of the sample. Since the net absorption is a sum of a large number of individual contributions, one can quote the central-limit theorem [4] to justify the Gaussian lineshape of EPR absorption lines. An excellent discussion of the underlying physical bases for the Gaussian and Lorentzian lineshapes is available [5].

Experimentally it is known that neither the Gaussian nor Lorentzian lineshape functions render a completely satisfactory description of the lineshape of an absorption

* Corresponding author. Fax: +306-966-4730.
E-mail address: john.weil@usask.ca (J.A. Weil).
[1] Present address. Department of Computer Science, 57 Campus Drive, University of Saskatchewan, Saskatoon, SK, Canada S7N 5A9.

1090-7807/03/$ - see front matter © 2003 Elsevier Science (USA). All rights reserved.
doi:10.1016/S1090-7807(02)00195-7

spectrum. The effect of rapid changes of the individual center's magnetization vectors can lead to a dynamic averaging of the individual distributions, leading again to a Lorentzian lineshape at the center while the wings of the line remain Gaussian. This effect is known as motional narrowing [6,7]. However, the main reason for failure of the Gaussian lineshape function is, in our opinion, the fact that the inhomogeneous broadening does not necessarily result in a Gaussian distribution of the net absorption.

There are few generalizations of these two lineshapes in the magnetic resonance literature. The Voigt lineshape function [8,9], a convolution of a Gaussian and a Lorentzian lineshape function, is a generalization of the above two approaches. Here the inhomogeneity is described by a Gaussian distribution of the line positions of individual centers, each contributing a Lorentzian-shape line to the spectrum. The superposition of these lines is described by the Voigt lineshape function. Both the Lorentzian and the Gaussian lineshapes are two special cases of this Voigtian lineshape. The first one occurs when the variance of the Gaussian distribution of line positions is zero (i.e., there is no inhomogeneity of the local magnetic fields), while the second takes place when the individual lines have zero linewidths (i.e., the Lorentzian lines are infinitesimally narrow and become Dirac delta distributions). Other attempts at lineshape functions include, for example, the use of Padé approximants [10,11], rational functions [12], and the heuristic lineshape function proposed by Więckowski [13].

A natural extension of the lineshape function is a Lévy distribution [14,15]. Here the Gaussian and Lorentzian lineshapes appear as two special cases. The non-Gaussian Lévy distributions arise as the limit distributions of the sums of independent random variables with infinite variance. However, the major disadvantage of the Lévy distributions is that, except for the two special cases, there is no analytical expression for these lineshape functions. Only the characteristic function of a general Lévy distribution can be expressed in a compact analytical form. Also the assumption that the variance of intensity is infinite is not really plausible. The truncated Lévy distributions [16] are an interesting modification of the Lévy distributions, having the property that the distribution wings decay exponentially, which guarantees that the variance and higher moments of these distributions are finite.

Another natural heuristic extension of the Gaussian and Lorentzian distributions are the distributions introduced by Tsallis [15]. Like the Lévy distributions, they include the Gaussian and Lorentzian lineshape functions as special cases. The advantage of the Tsallis distributions is that they have a simple analytic representation, with the Gaussian distribution being a pointwise limit of a sequence of Tsallis distributions.

The purpose of the present note is to study the applicability of Tsallis distributions for modeling the lineshape functions in continuous-wave EPR (and NMR) spectroscopy.

2. Tsallis lineshape functions

The distribution proposed by Tsallis was first derived as solutions to the generalized entropy-maximization principle [17,18]. After a suitable modification, in order to adapt the Tsallis distribution as a lineshape function $f_q(B)$, where B is the magnitude of field variable $\mathbf{B}$, it can be expressed as

$$f_q(B) = \left[1 + (2^{q-1} - 1)\left(\frac{B - B_r}{W}\right)^2\right]^{-(1/(q-1))}, \qquad (1)$$

where W is the half-width at half-height of f_q, and the parameter $q \in (1, \infty)$. For $q = 2$, this formula describes the Lorentzian lineshape function $(1 + (B - B_r)^2/W^2)^{-1}$. The definition of the lineshape function $f_q(B)$ can be extended to $[1, \infty)$ with $f_1(B)$ being the pointwise right-hand limit of $f_q(B)$ as $q \downarrow 1$ (i.e., as q decreases towards 1). This limit is the Gaussian lineshape function $\exp(-(\ln 2)(B - B_r)^2/W^2)$. There is no natural (i.e., smooth) extension of this lineshape function for q values smaller than 1, since the first right derivative $\mathrm{d}f_q(B)/\mathrm{d}q = +\infty$ at $q = 1$.

The function f_q as written in Eq. (1) is not normalized. For $1 < q < 3$, the normalization constant N_q is given by the expression

$$N_q = \int_{-\infty}^{\infty} f_q(B)\,\mathrm{d}B = \frac{W}{\sqrt{2^{q-1} - 1}}\beta\left(\frac{1}{2}, \frac{1}{q-1} - \frac{1}{2}\right), \qquad (2)$$

where $\beta(1/2, [\{1/(q-1)\} - (1/2)]$ is the Euler's integral of the first kind (β function) [19, Chapter 8.3]. The right-hand limit of the normalization constant N_q at $q = 1$ is $N_1 = \sqrt{(\ln 2)/(\pi W^2)}$ which is the normalization constant of the Gaussian lineshape function. Setting $z \equiv [\{1/(q-1)\} - (1/2)]$, the integral in Eq. (2) can be evaluated for every $z > 0$ (i.e., when $1 < q < 3$) using the series representation [19, Eqs. 8.382.3 and 8.384.1]

$$\beta\left(\frac{1}{2}, z\right) = \frac{1}{z} + \sum_{k=1}^{\infty} \frac{(2k-1)!!}{2^k k!}\frac{1}{z+k}. \qquad (3)$$

For $q \geqslant 3$, the integral in (2) becomes infinite. This means that the wings of the distribution (1) contain "almost all" the intensity. The normalized lineshape functions for various values of the parameter q are shown in Fig. 1.

The normalization constant (2) is the zeroth-order moment of the Tsallis distribution (1). In general, one can compute the nth order moment

$$M_n(q) \equiv \frac{1}{N_q}\int_{-\infty}^{\infty} (B - B_r)^n f_q(B)\,\mathrm{d}B. \qquad (4)$$

Since the function f_q is symmetric, all odd moments of the Tsallis distribution are 0. The even moments $M_n(\mathrm{q})$ are finite if the function $(B - B_r)^n f_q(B)$ decreases faster

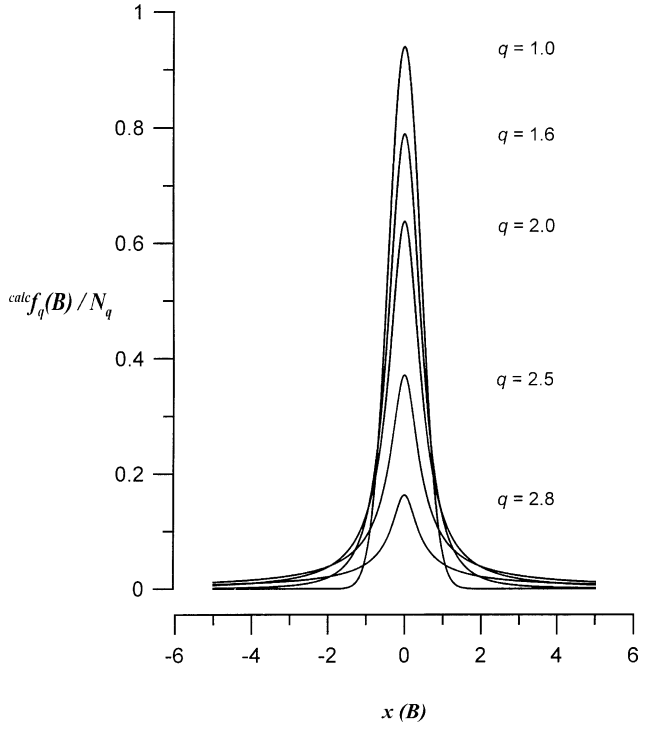

Fig. 1. Five normalized lineshape functions $f_q(B)$, with identical half-widths $2W = 1\,\mathrm{G}$ and identical resonance fields B_r, as functions of the argument $x = 2(B_\mathrm{r} - B)/W$ for five values of the parameter q. Here W is the half-width at half-height of the absorption curve f_q.

than $|B - B_\mathrm{r}|^{-1}$. This is equivalent to saying that q must obey the inequality

$$1 < q < \frac{n+3}{n+1}, \tag{5}$$

where n is any of the non-negative integers. Then

$$M_n(q) = \frac{1}{N_q}\left(\frac{W}{\sqrt{2^{q-1}-1}}\right)^{n+1}\beta\left(\frac{n+1}{2}, \frac{1}{q-1} - \frac{n+1}{2}\right). \tag{6}$$

In particular, the second moment is finite for $q < 5/3$, and the fourth moment is finite for $q < 7/5$. Hence, the ratio of the square of the squared second moment over the fourth moment can be computed for $1 < q < 7/5$, using the formula

$$\frac{M_2(q)^2}{M_4(q)} = \frac{1}{3}\left(\frac{1}{q-1} - \frac{5}{2}\right)\Big/\left(\frac{1}{q-1} - \frac{3}{2}\right). \tag{7}$$

The right-hand limit at $q = 1$ of this ratio is 1/3, which coincides with the value for the Gaussian lineshape [3, p. 1174].

The first derivative of the Tsallis lineshape function f_q with respect to B can be shown to be given by the expression

$$f_q'(B) = C(B_\mathrm{r} - B)\left[1 + (2^{q-1}-1)\left(\frac{B - B_\mathrm{r}}{W}\right)^2\right]^{-(q/(q-1))}, \tag{8}$$

where

$$C = \frac{2^{q-1}-1}{q-1}\frac{2}{W^2}$$

is a constant, i.e., is independent of the magnetic-field quantities. The right-hand limit of C at $q = 1$ is $(2\ln 2)/W^2$.

In the experimental realm, for EPR spectroscopy, the most readily accessible width parameter is the so-called peak-to-peak (first-derivative) linewidth ΔB_pp. It varies with the value of the parameter q and is known to be $(2/\sqrt{3})W$ for the Lorentzian lineshape and $(\sqrt{2/\ln 2})W$ for the Gaussian lineshape [20, Table E.1]. In general, within the range $(1, \infty)$ of q, the peak-to-peak width for the Tsallis lineshape can be obtained from the relation

$$\Delta B_\mathrm{pp} = 2W\left(\frac{q-1}{q+1}\frac{1}{2^{q-1}-1}\right)^{1/2}. \tag{9}$$

This expression reduces to the Lorentzian lineshape value at $q = 2$, and the right-hand limit of this expression at $q = 1$ is the Gaussian lineshape value.

A computer program (Simula) for simulation of simple EPR spectra using the Tsallis lineshape function has been written in C++ [21].

3. Examples

The examples shown below demonstrate how the Tsallis statistics can be used to better approximate the lineshape functions. All are drawn from X-band room-temperature EPR spectroscopy.

The best-fit spectrum corresponds to the minimum of the root-mean-square-error (rmse) between the amplitudes of the experimental ${}^{\exp}f_q'(B_i)$ and calculated ${}^{\mathrm{calc}}f_q'(B_i)$ first derivative of the EPR absorption line:

$$\mathrm{rmse} = \sqrt{\frac{1}{N}\sum_{i=1}^{N}\left[{}^{\exp}f_q'(B_i) - {}^{\mathrm{calc}}f_q'(B_i)\right]^2}. \tag{10}$$

Here the sum runs over all N experimental values of the magnetic field B_i $(i = 1, 2, \ldots, N)$ at which the line amplitudes $(f_q')^{\exp}(B_i)$ were recorded. The root-mean square error function is minimized with respect to all parameters of the theoretical lineshape. The root-mean-square (rms) of the experimental spectrum is defined as

$$\mathrm{rms} = \sqrt{\frac{1}{N}\sum_{i=1}^{N}\left[{}^{\exp}f_q'(B_i)\right]^2}. \tag{11}$$

Since the experimental amplitudes of different spectra are not consistently scaled, the ratio $R \equiv \mathrm{rmse}/\mathrm{rms}$ is reported in this paper. In the examples studied in this paper, the number of points $(B_i, {}^{\exp}f_q'(B_i))$ is $N = 1024$. We wish to note that in the following examples, we used

the same linewidth for all hyperfine components, i.e., assumed that width W is not appreciably a function of M_I, since we did not detect evidence experimentally for such an effect in our spectra.

In the first example, the first derivative of the *single* line arising from certain Gd^{3+} ($S = 7/2$) centers in single-crystal fluorapatite for the central set (six superimposed lines from the six symmetry-related sites) of transitions $M_S : +1/2 \leftrightarrow -1/2$, observed when $\mathbf{B}_{\|}$ crystal axis **c** [22, Note Fig. 4a therein]. Each of the six lines are expected to have identical parameters, except perhaps for a slight line-position difference, due to inevitable crystal misalignment (i.e., **B** deviates from **c**). All the other lines, which are far away, are ignored. The optimized parameters of the theoretical spectrum are the line position, the linewidth, the line intensity, and parameter q. Fig. 2 shows error ratio R plotted against q. The experimental spectrum and the best-fit Tsallian line are shown in Fig. 3.

The observed rather ill-defined minimum at $q = 2.3$ (Fig. 2) corresponds to a nearly Lorentzian lineshape. The fact that this minimum is shallow is not surprising. For sufficiently large values of q (i.e., $q > 2$), one could perhaps obtain a sharper minimum when using a wider spectral measurement range. The tails of the line are where the Tsallis distributions with various values of q can differ significantly, for $q > 2$. Of course, the signal-to-noise ratio may then cause a problem because the noise makes it difficult to obtain adequate data for the wings. In the immediate region around the minimum, for q larger than 2, the rms error obtained in fitting tends to be almost constant (see Fig. 2), but the resulting W is somewhat sensitive to the q value; the smaller the q value within this region, the larger is the W value obtained.

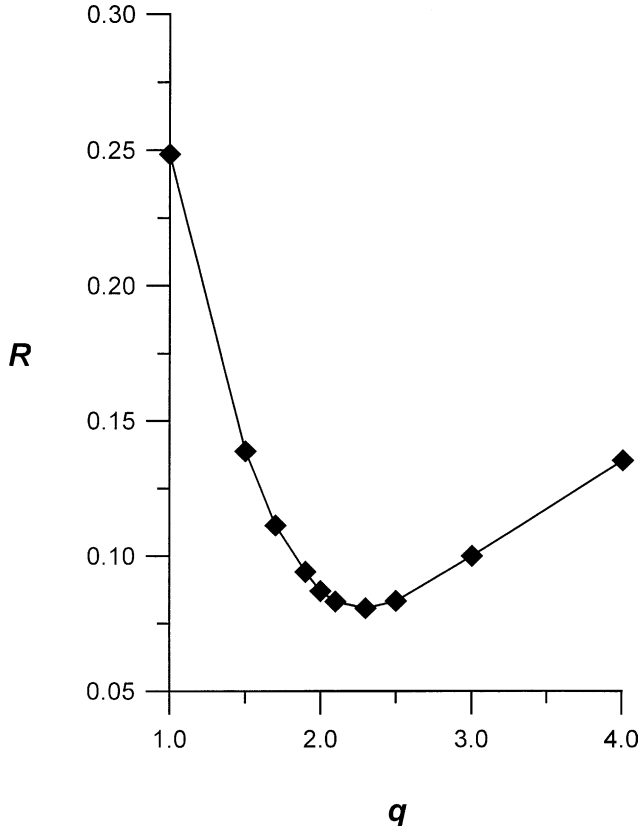

Fig. 2. Effect on the error ratio R of varying parameter q in the EPR lineshape fitting of Gd^{3+} [center '*a*', spin $S = 7/2$] in single-crystal fluorapatite for transition $M_S : +1/2 \leftrightarrow -1/2$, observed at room temperature when $\mathbf{B}\|\mathbf{c}$ [22]. The minimum in R occurs at $q = 2.3$ (see Fig. 3).

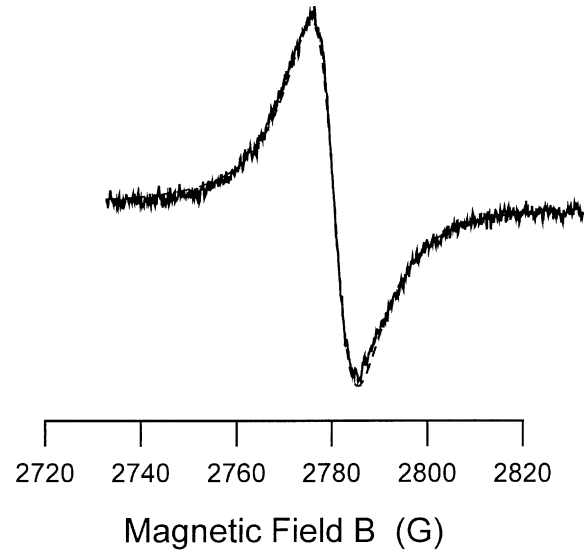

Fig. 3. The experimental and best-fit simulated EPR spectrum of Gd^{3+} [center '*a*'] in single-crystal fluorapatite for transition $M_S : +1/2 \leftrightarrow -1/2$, observed at 9.2 GHz and 300 K when $\mathbf{B}\|\mathbf{c}$ [22]. The simulated spectrum is represented by a dashed curve.

The second example is a spectrum of the free-radical salt (1,1-diphenylhydrazinium$^+$) 2,2-diphenyl-1-(2,6-dinitro-4-sulfophenyl)hydrazyl$^{\bullet-}$ in H_2O [23]. The error ratios R calculated using different lineshape functions are shown in Fig. 4. Here again all optimization was done for all parameters of this line: the position of the spectrum center, the two isotropic hyperfine splitting constants for the two nitrogen ^{14}N nuclei, the (single) linewidth, the line intensity, and the parameter q. The minimum in R is found to occur at or very close to 1, that is, at the end of the interval of the allowed values of q. This value corresponds to the Gaussian lineshape. The experimental and simulated spectra are shown in Fig. 5.

As a third example, in Fig. 6, the experimental and simulated EPR spectra of the free radical 2,2-diphenyl-1-picrylhydrazyl (DPPH$^{\bullet}$) at various concentrations in liquid benzene are shown. The optimized parameters (except for the position of the spectrum center) for the simulated spectra are collected in Table 1. In these calculations, the 2nd-order hyperfine corrections [20, Eq. 3.2], being of order 0.01 G, have been neglected. One can

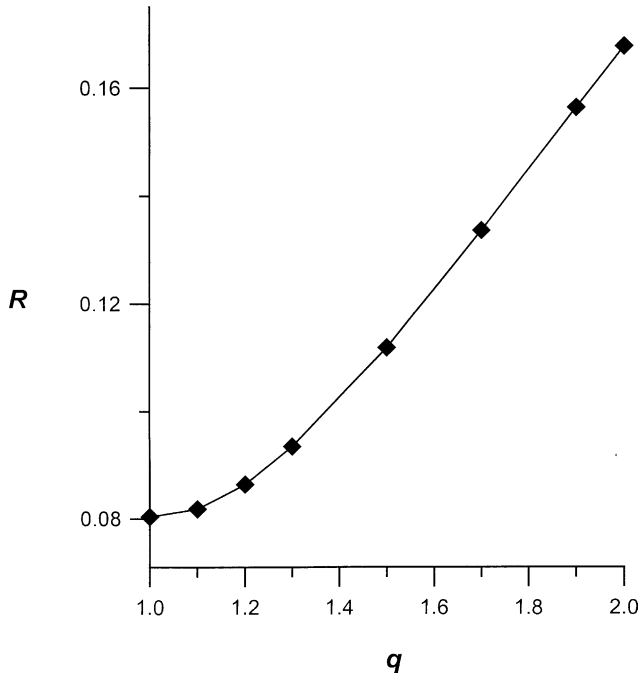

Fig. 4. Effect on the error ratio R of varying parameter q in the lineshape fitting. In this study, a room-temperature aqueous solution EPR spectrum (taken @ 9.3998 GHz) of the free-radical salt (1,1-diphenylhydrazinium^{+}) 2,2-diphenyl-1-(2,6-dinitro-4-sulfophenyl)hydrazyl$^{\cdot -}$ in water solution was used, at concentration $\sim 10^{-5}$ M (see Fig. 5).

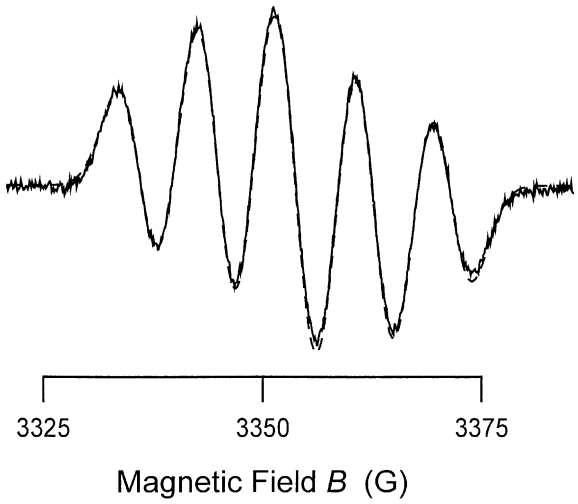

Fig. 5. The experimental and simulated EPR spectra (@ 9.3998 GHz) of the free-radical salt (1,1-diphenylhydrazinium^{+}) 2,2-diphenyl-1-(2,6-dinitro-4-sulfophenyl)hydrazyl$^{\cdot -}$ in water solution at room-temperature [23]. The five lines arise from the hyperfine interactions of the unpaired-electron spin with the two almost equivalent hydrazinic nitrogen nuclei (^{14}N, nuclear spin 1) of the anion. The presence of dioxygen in the solution and the modulation amplitude used (1 G) precluded resolution of the ^{1}H super-hyperfine structure. The simulated spectrum is represented by a dashed curve.

see that as the concentration of DPPH$^{\cdot}$ increases, the original hyperfine structure of the spectrum disappears and a single broadened line of nearly Lorentzian shape ($q = 1.9$) emerges. This can be explained by inhomogeneous broadening due to intermolecular magnetic dipole interactions, while the Lorentzian lineshape can be attributed to the intermolecular spin exchange [5,6]. Both manifest themselves at sufficiently high DPPH$^{\cdot}$

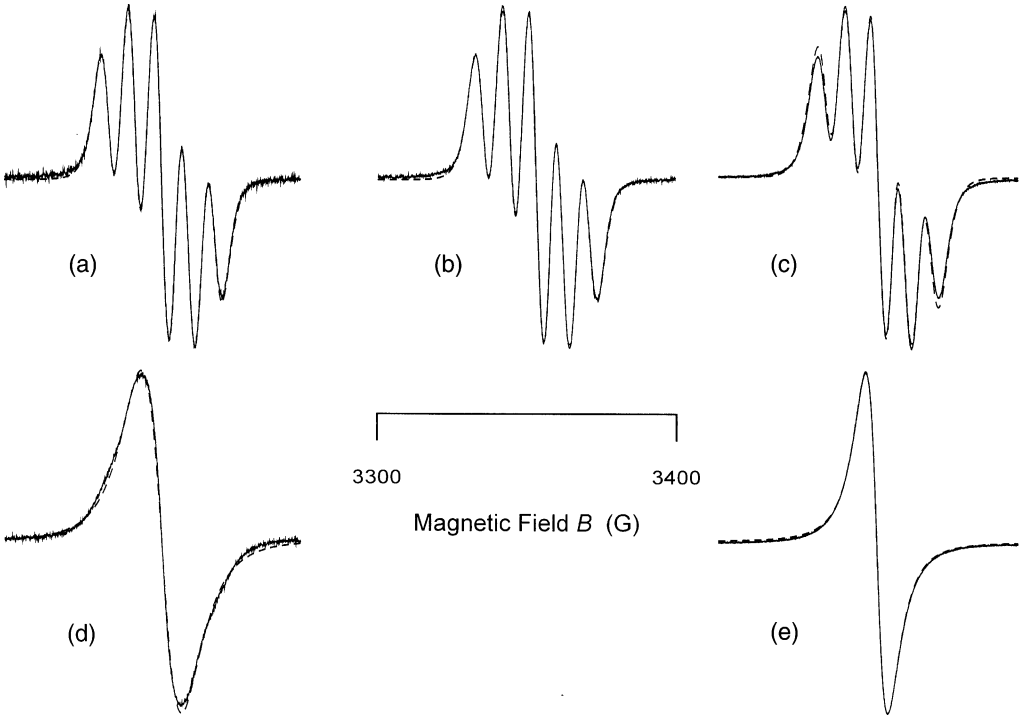

Fig. 6. The experimental and simulated (dashed curves) EPR spectra (@ ca. 9.40 GHz) of DPPH$^{\cdot}$ radical in benzene solution (room T, in air) at various concentrations of this free radical: (a) 1.0×10^{-4} M; (b) 1.0×10^{-3} M; (c) 1.0×10^{-2} M; (d) 5.0×10^{-2} M; (e) 1.0×10^{-1} M. The parameters for the simulated spectra are listed in Table 1.

Table 1
The optimal parameters for the simulated EPR spectra of DPPH· in benzene solution at various concentrations of this free radical, as shown in Fig. 6

Radical concentration (M)	q (unitless)	$2W$ (G)	^{14}N hyperfine splitting factors (G)		R (unitless)
			$A_1/g_e\beta_e$	$A_2/g_e\beta_e$	
1.0×10^{-4}	1.32	8.1_8	8.07	9.59	0.04
1.0×10^{-3}	1.31	8.0_7	8.07	9.61	0.03
1.0×10^{-2}	1.29	9.0_1	8.13	9.15	0.06
5.0×10^{-2}	1.63	20.5_1	—	—	0.05
1.0×10^{-1}	1.90	12.7_8	—	—	0.01

The experimental spectra were recorded in the presence of dissolved air (i.e., di-oxygen). The magnetic field was modulated at 50 kHz, with amplitude 0.996 G.

The numerical precision of each lineshape parameter is determined by the magnitude of the iteration steps selected for the optimization. The EPR parameters (i.e., W, A_1, and A_2) were calculated using 0.01 G at each successive fitting. The lineshape parameter q was optimized using 0.01 as the interval. Since the computational algorithm used to determine R of each simulated spectrum is relatively insensitive to changes in W as compared to changes in the A values, the optimized line width is not considered to be as accurate.

concentrations (greater than 0.05 M). At lower DPPH· concentrations (less than 0.01 M) the hyperfine components of the spectrum are clearly visible and the individual line shape becomes close ($q = 1.3$) to the Gaussian lineshape due to the largely concentration-independent local-field inhomogeneity (unresolved hyperfine splittings). In an earlier investigation [24], good fits were obtained with Gaussian lineshapes, but using very slight differences in linewidths for the components. This was attributed to incomplete averaging of the hyperfine anisotropy. In our, work, we did not find it necessary to use M_I-dependent widths.

4. Conclusion

In this contribution, we have proposed using the new lineshape function derived by Tsallis [17] to simulate EPR spectra. This new symmetric function includes the Gaussian and Lorentzian lineshape functions as special cases. In addition to the linewidth parameter, the shape of the line is controlled by one more parameter (q) that determines the contribution of the line wings to the integral intensity. We have produced a number of simulations showing that the new lineshape function is useful and can improve the quality of simulated spectra. The results also suggest that the parameter q may possibly be interpreted as a measure of the strength of the spin exchange present [6]. Thus $q = 1$, the lowest value of q, may correspond to the lack of such exchange. For instance, see above, as the concentration of DPPH· free radicals increases, the best-fit values of q increase as well (Table 1). Hence the idea that the changes in q reflect the changes in the effectiveness of exchange interactions. It is not the purpose of the present work to assess the theoretical basis of parameter q (and of parameter W), especially since the contributions encountered depend sensitively on the physical system studied.

In closing, we wish to point out that the Tsallian lineshape can of course also be used to simulate powder envelopes. To be sure, there is the likelihood that q can depend on the field position (crystallite orientation), just as width W does. It is known that the first-derivative powder pattern "integrates" the spectrum [25], so that the end features in it reproduce the actual absorption shapes, e.g., Tsallian peaks.

Acknowledgments

The authors thank to Dr. Ning Chen and Ms. Monika D. Lafond for providing us with useful spectra, and to Dr. Mark J. Nilges and Mr. Brett A. Rogers for helpful comments and discussions

References

[1] J.A. Weil, The simulation of EPR spectra: a mini-review, Mol. Phys. Rep. 26 (1999) 11.
[2] R. Kubo, A general theory of magnetic resonance absorption, J. Phys. Soc. Jpn. 9 (1954) 888.
[3] J.H. Van Vleck, The dipolar broadening of magnetic resonance lines in crystals, Phys. Rev. 74 (1948) 1168.
[4] W. Feller, An Introduction to Probability Theory and its Applications, Wiley, New York, 1971.
[5] O. Svelto, in: Principles of Lasers, fourth ed., Plenum Press, New York, 1998, pp. 31–50.
[6] P.W. Anderson, P.R. Weiss, Exchange narrowing in paramagnetic crystals, Rev. Mod. Phys. 25 (1953) 269.
[7] P.W. Anderson, A mathematical model for the narrowing of spectral lines by exchange motion, J. Phys. Soc. Jpn. 9 (1954) 316.
[8] W. Voigt, Über die Intensitätsverhaltung innerhalb einer Spektrallinie, Phys. Z. 14 (1913) 377.
[9] J.-P. Grivet, Accurate numerical approximation to the Gauss–Lorentz lineshape, J. Magn. Reson. 125 (1997) 102–106.
[10] L.I. Antsiferova, E.V. Valova, New approach to calculating the ESR spectra with allowance for the effects of saturation and modulation effect, Khim. Fiz. 16 (1997) 37–47.
[11] T. Czosnyka, A. Trzcińska, Unified analytical approximation of Gaussian and Voigtian lineshapes, Nucl. Instrum. Methods Phys. Res. A 431 (1999) 548.

[12] M.M. Maltempo, Rational function approximations to generalized spectroscopic lineshapes and applications to electron paramagnetic resonance, J. Magn. Reson. 68 (1986) 102.
[13] A.B. Więckowski, Numerical methods in line-shape analysis, Nukleonika 42 (1997) 589.
[14] B.V. Gnedenko, A.N. Kolmogorov, Limit Distributions for Sums of Independent Random Variables, Addison-Wesley, Cambridge, MA, 1954.
[15] C. Tsallis, S.V.F. Lévy, A.M.C. Souza, R. Maynard, Statistical–mechanical foundation of the ubiquity of Lévy distributions in nature, Phys. Rev. Lett. 75 (1995) 3589.
[16] I. Koponen, Analytic approach to the problem of convergence to truncated Lévy flights towards the Gaussian stochastic process, Phys. Rev. E 52 (1995) 1197.
[17] C. Tsallis, Possible generalization of Boltzmann–Gibbs statistics, J. Stat. Phys. 52 (1988) 479.
[18] C. Tsallis, Lévy distributions, Phys. World 10 (1997) 42.
[19] I.S. Gradshteyn, I.M. Ryzhik, Tables of Integrals, Series, and Products, Academic Press, New York, 1965.
[20] J.A. Weil, J.R. Bolton, J.E. Wertz, Electron Paramagnetic Resonance. Elementary Theory and Applications, Wiley, New York, 1994.
[21] Simula1, v4, EPR Research Group, University of Saskatchewan, Saskatoon, Canada, 2002. This program is available via Website: http://chm15127.usask.ca/.
[22] N. Chen, Y. Pan, J.A. Weil, Electron paramagnetic resonance spectroscopic study of synthetic fluorapatite: Part I. Local structural environment and substitution mechanism of Gd^{3+} at the Ca2 site, Am. Miner. 87 (2002) 37.
[23] D.F. Howarth, M.D. Lafond, J.A. Weil, A liquid-solution EPR study of 2,2-diphenyl-1-monosulfodinitrophenyl hydrazyl salts, Can. J. Chem. (2003), to be submitted.
[24] A. Mąkosa, A broadening effect of hyperfine structure lines in DPPH electron spin resonance spectrum, Acta Phys. Polon. A 39 (1971) 161.
[25] J.A. Weil, H.G. Hecht, On the powder line shape of EPR spectra, J. Chem. Phys. 38 (1963) 281.